

8-2007

# Exact Solution of Time History Response for Dynamic Systems with Coupled Damping using Complex Mode Superposition

Manoj kumar Chinnakonda  
Clemson University, mchinna@clemson.edu

Follow this and additional works at: [https://tigerprints.clemson.edu/all\\_theses](https://tigerprints.clemson.edu/all_theses)

 Part of the [Engineering Mechanics Commons](#)

---

## Recommended Citation

Chinnakonda, Manoj kumar, "Exact Solution of Time History Response for Dynamic Systems with Coupled Damping using Complex Mode Superposition" (2007). *All Theses*. 207.  
[https://tigerprints.clemson.edu/all\\_theses/207](https://tigerprints.clemson.edu/all_theses/207)

This Thesis is brought to you for free and open access by the Theses at TigerPrints. It has been accepted for inclusion in All Theses by an authorized administrator of TigerPrints. For more information, please contact [kokeefe@clemson.edu](mailto:kokeefe@clemson.edu).

EXACT SOLUTION OF TIME HISTORY RESPONSE  
FOR DYNAMIC SYSTEMS WITH COUPLED DAMPING  
USING COMPLEX MODE SUPERPOSITION

---

A Thesis  
Presented to  
the Graduate School of  
Clemson University

---

In Partial Fulfillment  
of the Requirements for the Degree  
Master of Science  
Mechanical Engineering

---

by  
Manoj Kumar M Chinnakonda  
August 2007

---

Accepted by:  
Dr. Lonny L. Thompson, Committee Chair  
Dr. Paul F. Joseph  
Dr. Ardalan Vahidi

## ABSTRACT

An exact solution method for general, non-proportional damping time history response for piece-wise linear loading proposed by Dickens is generalized to piece-wise quadratic loading. Comparisons are made to Trapezoidal and Simpson's quadrature rules for approximating the time integral of the weighted generalized forcing function in the exact solution to the decoupled modal equations arising from state-space modal analysis of linear dynamic systems. The time integral of the forcing function is recognized as a weighted integral with complex exponential and the general update formulas are derived using polynomial interpolation to the forcing function. Closed-form expressions for the weighting parameters in the quadrature formulas in terms of time-step size and complex eigenvalues are derived. The solution is obtained step-by-step from update formulas obtained from the piecewise linear and quadratic interpolatory quadrature rules starting from the initial conditions. Linear approximation for loading within a time-step used by Dickens is shown to be a special case of the quadrature rules with linear interpolation. The solution methods are exact for piecewise linear and quadratic loading with or without initial conditions and are computationally efficient with low memory for time-history response of linear dynamic systems including general non-proportional viscous damping. An examination of error estimates for the different force interpolation methods shows convergence rates depend explicitly on the amount of damping in the system as measured by the real-part of the complex eigenvalues of the state-space modal equations and time-step size. Numerical results for a system with general, non-proportional damping, and driven by a continuous loading shows that for systems with light damping, update formulas for standard Trapezoidal and Simpson's rule integration have comparable accuracy to the weighted piecewise linear and quadratic force interpolation update

formulas, while for heavy damping, the update formulas from the weighted force interpolation quadrature rules are more accurate. Using a simple model representing a stiff system with general damping, a two-step modal analysis using real-valued modal reduction followed by state-space modal analysis is shown to be an effective approach for rejecting spurious modes in the spatial discretization of a continuous system.

## DEDICATION

I dedicate this work to my dad Dr. C.C. Mohan Ram (late), my mom Mrs. Uma Mohan and my beloved brother Madhan for their love and support.

## ACKNOWLEDGMENTS

I would like to express my deepest gratitude to Dr. Lonny L. Thompson, my research advisor, for this excellent guidance throughout my Master's at Clemson. His invaluable support and inputs have helped me reach a much higher platform of knowledge both in Mechanical Engineering and as an individual.

I would like to thank Dr. Paul F. Joseph and Dr. Ardalan Vahidi for agreeing to be in my committee.

Next, I would like to specially thank my soul mate and girl friend Priya for being there for me whenever needed.

Finally, I would like to mention a special thanks to my project mate Abhinand for nurturing a healthy and learning work environment and also my room mates Bala and Vedik and my lab mates for their help and guidance.

## TABLE OF CONTENTS

	Page
TITLE PAGE . . . . .	i
ABSTRACT . . . . .	ii
DEDICATION . . . . .	iv
ACKNOWLEDGMENTS . . . . .	v
LIST OF FIGURES . . . . .	vii
CHAPTER	
1. INTRODUCTION . . . . .	1
2. MODAL ANALYSIS FORMULATION . . . . .	7
3. NUMERICAL EXAMPLES . . . . .	19
4. CONCLUSIONS . . . . .	32
APPENDIX: EXACT SOLUTION FOR LINEAR INTERPOLATION FORCING FUNCTIONS . . . . .	35
BIBLIOGRAPHY . . . . .	38

## LIST OF FIGURES

Figure	Page
3.1 Numerical example with non-proportional damping setup. . . . .	19
3.2 Displacements for Masses 1 and 2 with non-proportional light damping	21
3.3 Error in Displacements for Mass-1 with light damping. . . . .	21
3.4 Error in Displacements for Masses 1 and 2 and light damping . . . . .	22
3.5 Displacements for Masses 1 and 2 with very heavy non-proportional damping . . . . .	23
3.6 Error in Displacements with very heavy non-proportional damping . . .	24
3.7 Error versus non-proportional damping measured by $0 \leq c \leq 4\pi$ . . . . .	25
3.8 Error versus time-step size for Mass-1, (a) light damping, (b) very heavy damping . . . . .	26
3.9 Displacements for Mass-1 and Mass-2 comparing P1 method with Exact solution subject to initial conditions for light damping . . . . .	27
3.10 Results from stiff spring-mass system with damping . . . . .	29



CHAPTER 1  
INTRODUCTION

Discrete dynamic systems such as in structural dynamics with mass, stiffness and damping can be described by a coupled system of second-order ordinary differential equations in time for the displacement vector  $\mathbf{u}(t)$  of dimension  $N$  such that

$$\mathbf{M}\ddot{\mathbf{u}}(t) + \mathbf{C}\dot{\mathbf{u}}(t) + \mathbf{K}\mathbf{u}(t) = \mathbf{f}(t), \quad t \in (0, t_f), \quad (1.1a)$$

$$\mathbf{u}(0) = \mathbf{u}_0, \quad (1.1b)$$

$$\dot{\mathbf{u}}(0) = \mathbf{v}_0, \quad (1.1c)$$

In the above, a superdot denotes differentiation with respect to time,  $\mathbf{f}(t)$  is the prescribed load vector, and  $\mathbf{u}_0$  and  $\mathbf{v}_0$  are the initial displacement and velocity vectors, respectively. The matrices are real-valued and symmetric; the mass matrix  $\mathbf{M}$  is symmetric positive-definite, while the damping matrix  $\mathbf{C}$  and stiffness matrix  $\mathbf{K}$  are symmetric and semi-positive-definite.

This system of coupled ordinary differential equations in time can be solved directly using direct time-integration methods which approximate derivatives with difference equations. Both explicit or implicit time-stepping approximation methods may be used such as central difference or single-step/single-solve average acceleration schemes [1]. Although explicit methods are computationally efficient, their solutions are only conditionally stable by a restriction on the maximum time step size. Unconditionally stable implicit algorithms have no stability restrictions when applied to linear problems but require the solution of a coupled matrix equation system of size  $N$  at each time step. These algorithms may be unsatisfactory for long-term simulations where excessive accumulation error over long time intervals with many small

time steps may occur. For problems with sufficient regularity, high-order accurate algorithms which allow a larger time step size without compromising efficiency or accuracy for long-time solutions are preferred, see e.g. [2, 3].

For linear systems, the time-response can be computed using mode superposition techniques. Classical modal methods solve a real-valued eigenproblem for real valued natural frequencies (eigenvalues) and mode shapes (eigenvectors). The orthogonal properties of these mode shapes are then used with superposition and a normal mode transformation to diagonalize the mass and stiffness matrices. For general, non-proportional damping matrices, using the real modes of the stiffness and mass in a normal mode transformation, the modal damping matrix remains coupled. Often, a diagonal modal damping matrix is assumed by neglecting the off-diagonal terms, assuming damping is proportional to mass and stiffness matrices, or approximating diagonal modal damping from an experimental modal survey. For systems with localized viscoelastic isolation systems or localized discrete viscous dampers, as is often the case in practice, the damping will be non-proportional and classical modal analysis which neglects non-proportional damping can lead to incorrect and misleading solutions for the predicted dynamic response [4, 5, 6]. Several techniques have been proposed for measuring non-proportional physical and corresponding modal damping matrices from experiments, see e.g. [7, 8]. Indices measuring the damping non-proportionality have also been proposed by several authors, e.g. [9, 10]. Quantification of the non-proportionality of damping is important in modal testing, and model correlation.

### Literature Review

Various techniques are followed in the way non-proportional damping is handled while solving dynamic system of equations. In [5], the nondiagonal terms in the

modal damping matrix are moved to the right-hand-side as a pseudo-load term proportional to the cross-coupling damping matrix times the generalized velocity vector after modal transformation, leaving on the left-hand-side pseudo-uncoupled equations with modal damping ratios. An approximate solution to these pseudo-uncoupled equations is obtained by assuming piecewise linear functions in time for both the generalized forcing function and modal velocities in the pseudo-load term multiplying the cross-coupling damping matrix. The resulting scheme requires a matrix inversion with operation count of approximately the cube of the number of retained real modes and is not exact because of the linear approximations. Alternatively, Picard iteration can be used to solve the pseudo-uncoupled equations, see [11] and others.

An alternative is to express the dynamic equations in state-space form and solve the complex eigenproblem of size  $2N$  which includes the arbitrary damping matrix. The resulting orthogonal complex modes when used with a complex mode superposition (complex mode transformation) result in fully decoupled modal equations [12]. The exact solution to the complex modal equations involves an integral over time of the generalized forcing function weighted by a complex exponential [13]. A well-known approximation leading to update recurrence formulas at time steps is to approximate the load with an impulse response function or a constant at the beginning of each step, see e.g. [14]. In [15], the generalized forcing function in the complex modal equations are approximated by a piecewise linear loading. The particular solution for the linear approximation of the loading within a time-step is then derived in closed-form. The result is a time-stepping method which includes general, non-proportional damping and is exact for piecewise linear loading. Update formulas for real-valued modal analysis with proportional damping which are exact for piecewise linear loading are summarized in [16]. The modal analysis methods are computationally efficient with limited memory or disk requirements provided the complex eigensolution of size  $2N$  can be amortized over time-steps. Physical space

counter-parts of the constant and linear force modal update formulas involve direct discrete-transition matrices in terms of the matrix exponential of the state-space matrix [17, 14]. This alternative discrete-time transition approach requires evaluation of the exponential state-space matrix usually obtained by a direct Taylor-series expansion with scaling used to speed convergence [18]. The cost of solving the complex eigenvalue problem in the modal approach is balanced by the significantly smaller effort required to compute the modal update formulas than to directly compute the exponential state-space matrix.

### Thesis Goals and Objectives

The goal of this thesis is to evaluate the state-space modal analysis method for non-proportional damping time history response proposed by Dickens [15] for piecewise linear load and compare the solution to its alternatives, including trapezoidal and high-order Simpson's quadrature rules for approximating the time integral of the weighted forcing function in the exact solution to the decoupled complex modal equations.

In this work, the interpolatory quadrature rules are to be derived using high-order (linear and quadratic) interpolation of the discrete forcing data followed by closed-form expressions for the weighting parameters in the quadrature formulas in terms of time-step size and complex eigenvalues by assuming that the forcing functions are known at discrete time-steps. Update formulas are to be derived from the interpolatory quadrature rules, which can be used to develop the complex valued modal solution step-by-step from the initial condition until the final time of interest is reached.

In addition, it is also intended to compare linear and quadratic interpolatory algorithms with trapezoidal and high-order Simpson's quadrature rules using numerical examples which demonstrate the accuracy and convergence rates of the methods

showing comparisons between a range of light and heavy non-proportional viscous damping and also the effectiveness of modal reduction to eliminate any spurious modes in stiff systems.

### Thesis Outline

Chapter 2 elaborates the modal analysis formulation technique in which derivation of complex uncoupled modal equations starting from general coupled discrete dynamic system of equations is detailed, taking into account the method of retaining certain number of modes to reject spurious modes from stiff systems. Following modal analysis, the method of obtaining the update formulas used in interpolatory quadrature rules is shown.

Initially, real eigen analysis is carried out using the mass and stiffness matrices of the coupled discrete dynamic system in order to identify the real eigenvalues (natural frequencies) and eigenvectors (mode shapes). Using mode superposition of these orthonormal eigenvectors, the normal mode transformation is used to reduce the general coupled discrete dynamic system equations of motion to a system of modal differential equations. The technique of moving the non-diagonal coefficients of the normal transformed damping matrix to the right-hand-side and the methods of solving the pseudo-decoupled modal differential equations are then discussed.

As an alternative to moving the cross-coupling terms from the transformed damping matrix to the right-hand-side, the modal differential equations are cast in state-space form and the concepts of complex eigen analysis are introduced. It is then shown how the state-space transformed modal equations are decoupled using complex transformation resulting in uncoupled modal equations for the complex valued function excited by a generalized forcing function.

Chapter 2 then focuses on derivation of the update formulas used for linear, quadratic, trapezoidal and Simpson's interpolatory quadrature rules. From the explicit integral solution of the uncoupled modal equations in complex domain, it is shown in detail how the update formulas are obtained for linear and quadratic approximations for the generalized force prescribed at discrete points using Lagrangian interpolation functions followed by trapezoidal and Simpson's quadrature rules which approximate the integrand (forcing function multiplied by an exponential term) as a whole.

Numerical examples are described in Chapter 3 that help support the theory developed and also compare the various interpolatory quadrature rules discussed in previous chapters. The physical setup of the numerical problem is described comprising of a two degree of freedom mass-spring-damper system excited by sinusoidal forcing functions. First, a sensitivity analysis is made on the results obtained by varying the amount of damping in the system followed by convergence studies of the various interpolatory quadrature rules discussed earlier. The linear interpolatory quadrature rule developed is then compared with HHT- $\alpha$  [19] method for spurious mode rejection for stiff systems and the results are discussed in detail.

Chapter 4 concludes the thesis by summarizing the theory developed in solving the general non-proportionally damped discrete dynamic systems using state-space transformation technique the results obtained through the numerical examples for convergence study and effective spurious mode rejection and finally outlines key avenues identified for future work.

CHAPTER 2  
MODAL ANALYSIS FORMULATION

Consider the generalized real eigenvalue problem neglecting damping,

$$(\mathbf{K} - \omega_i^2 \mathbf{M})\boldsymbol{\varphi}_i = \mathbf{0}$$

Since  $\mathbf{K}$  and  $\mathbf{M}$  are symmetric and positive, the undamped natural frequencies  $\omega_i \geq 0$ ,  $i = 1, 2, \dots, N$  are real, positive, and distinct. The associated eigenvectors  $\boldsymbol{\varphi}_i$  are orthonormal and assumed scaled such that  $\mathbf{P}^T \mathbf{M} \mathbf{P} = \mathbf{I}$ , and  $\mathbf{P}^T \mathbf{K} \mathbf{P} = \boldsymbol{\Omega}$  where  $\mathbf{P} = [\boldsymbol{\varphi}_1, \boldsymbol{\varphi}_2, \dots, \boldsymbol{\varphi}_N]$  is the matrix formed by columns filled with the eigenvectors, and  $\boldsymbol{\Omega} = \text{diag}(\omega_1^2, \omega_2^2, \dots, \omega_N^2)$  is the diagonal matrix of eigenvalues. Using a linear combination of the orthonormal eigenvectors defined by a mode superposition, the modal transformation

$$\mathbf{u}(t) = \sum_{j=1}^N \boldsymbol{\varphi}_j q_j(t) = \mathbf{P} \mathbf{q}(t) \quad (2.1)$$

reduces (1.1) to the system of modal differential equations of motion

$$\ddot{\mathbf{q}}(t) + \mathbf{C}^* \dot{\mathbf{q}}(t) + \boldsymbol{\Omega} \mathbf{q}(t) = \mathbf{Q}(t) \quad (2.2)$$

with initial conditions  $\mathbf{q}(0) = \mathbf{P}^T \mathbf{M} \mathbf{u}_0 = \tilde{\mathbf{u}}_0$ ,  $\dot{\mathbf{q}}(0) = \mathbf{P}^T \mathbf{M} \mathbf{v}_0 = \tilde{\mathbf{v}}_0$ , where

$$\mathbf{Q} = \mathbf{P}^T \mathbf{F}$$

$$\mathbf{C}^* = \mathbf{P}^T \mathbf{C} \mathbf{P}$$

is generally coupled for non-proportional damping; each mode is coupled to every other mode due to the off-diagonal damping terms. When the dynamic response is substantially contained in the lower modes, a reduced number of modes  $N_r \leq N$  in the modal transformation may be retained and the higher order modes are neglected

to provide efficiency. Pseudo-uncoupled modal equations can be obtained by moving the non-diagonal coefficients of  $\mathbf{C}^*$  to the right-hand-side, with the result

$$\ddot{\mathbf{q}}(t) + 2\xi\Omega\dot{\mathbf{q}}(t) + \Omega\mathbf{q}(t) = \mathbf{Q}(t) - \mathbf{X}\dot{\mathbf{q}}(t) \quad (2.3)$$

where  $\mathbf{X} = \text{nondiag}(\mathbf{C}^*)$  is the modal cross-coupling damping matrix and  $2\xi\Omega = \text{diag}(\mathbf{C}^*)$  where  $\xi$  is the diagonal matrix of modal damping ratios. In general,  $\mathbf{X}$  is not equal to 0. Solutions to (2.3) can be obtained iteratively using Picard iteration [11] or approximated by assuming piecewise linear functions in time for both  $\mathbf{Q}(t)$  and modal velocities  $\dot{\mathbf{q}}(t)$  in the psuedo-load term multiplying  $\mathbf{X}$  on the right-hand-side and integrating the analytical solution over a time-step [5]. The resulting scheme requires a matrix inversion with operation count of approximately the cube of the number of retained real modes and is not exact because of the linear approximations [11].

Alternatively, the second-order modal differential equations (2.2) can be cast in state-space form as a first-order system of size twice the number of retained real modes.

$$\hat{\mathbf{M}}\dot{\mathbf{x}} + \hat{\mathbf{K}}\mathbf{x} = \hat{\mathbf{Q}}(t) \quad (2.4)$$

$$\mathbf{x}(0) = [\tilde{\mathbf{v}}_0; \tilde{\mathbf{u}}_0] \quad (2.5)$$

where  $\mathbf{x}(t) = [\dot{\mathbf{q}}; \mathbf{q}]$ ,  $\hat{\mathbf{Q}} = [\mathbf{0}; \mathbf{Q}]$  and

$$\hat{\mathbf{M}} = \begin{bmatrix} \mathbf{0} & \mathbf{I} \\ \mathbf{I} & \mathbf{C}^* \end{bmatrix}, \quad \hat{\mathbf{K}} = \begin{bmatrix} -\mathbf{I} & \mathbf{0} \\ \mathbf{0} & \Omega \end{bmatrix}$$

Since  $\hat{\mathbf{M}}$  and  $\hat{\mathbf{K}}$  contain only real numbers, for the eigenvalues  $\hat{\lambda}_k$  which occur as complex numbers, the eigenvalues and associated orthogonal eigenvectors  $\boldsymbol{\psi}_j$  in the problem  $(\hat{\mathbf{K}} - \hat{\lambda}_j\mathbf{I})\boldsymbol{\psi}_j = \mathbf{0}$  occur in conjugate pairs. The matrices  $\hat{\mathbf{M}}$  and  $\hat{\mathbf{K}}$  are also symmetric which can be taken advantage to solve the eigenvalue problem efficiently.



Using the transformation  $\mathbf{x}(t) = \boldsymbol{\Psi}\mathbf{g}(t)$  where  $\boldsymbol{\Psi}$  is the normalized eigenvector matrix satisfying  $\boldsymbol{\Psi}^T \hat{\mathbf{M}} \boldsymbol{\Psi} = \mathbf{I}$ , and  $\boldsymbol{\Psi}^T \hat{\mathbf{K}} \boldsymbol{\Psi} = \hat{\boldsymbol{\Lambda}} = \text{diag}(\hat{\lambda}_1, \hat{\lambda}_2, \dots, \hat{\lambda}_{2N_r})$  in (2.4) leads to the uncoupled modal equations for the complex-valued functions  $\mathbf{g}(t)$

$$\dot{\mathbf{g}}(t) + \hat{\boldsymbol{\Lambda}}\mathbf{g}(t) = \mathbf{G}(t) \quad (2.6)$$

with generalized forcing function  $\mathbf{G} = \boldsymbol{\Psi}^T \hat{\mathbf{Q}}$  and with initial conditions  $\mathbf{g}(0) = \boldsymbol{\Psi}^T \hat{\mathbf{M}} \mathbf{x}(0)$ .

When the number of real modes retained  $N_r$  is equal to the number of original discrete equations  $N$ , a system of uncoupled complex modal equations can be obtained directly by defining  $\mathbf{v}(t) = \dot{\mathbf{u}}(t)$ , and writing the original equations of motion (1.1) in state-space form as [20]:

$$\mathbf{B}\dot{\mathbf{y}}(t) + \mathbf{A}\mathbf{y}(t) = \mathbf{R}(t) \quad (2.7a)$$

$$\mathbf{y}(0) = [\mathbf{v}_0; \mathbf{u}_0], \quad (2.7b)$$

where

$$\mathbf{A} = \begin{bmatrix} -\mathbf{M} & \mathbf{0} \\ \mathbf{0} & \mathbf{K} \end{bmatrix}, \quad \mathbf{B} = \begin{bmatrix} \mathbf{0} & \mathbf{M} \\ \mathbf{M} & \mathbf{C} \end{bmatrix},$$

$$\mathbf{y}(t) = \begin{Bmatrix} \mathbf{v}(t) \\ \mathbf{u}(t) \end{Bmatrix}, \quad \mathbf{R}(t) = \begin{Bmatrix} \mathbf{0} \\ \mathbf{F}(t) \end{Bmatrix}. \quad (2.8)$$

For the eigenvalues  $\lambda_j$  which occur as complex numbers, the complex eigenvalues and associated orthonormal eigenvectors  $\mathbf{V}_j$  in the problem  $(\mathbf{A} - \lambda_j \mathbf{I})\mathbf{V}_j = \mathbf{0}$  occur in complex conjugate pairs. Using the transformation  $\mathbf{y}(t) = \mathbf{V}\mathbf{z}(t)$  where  $\mathbf{V}$  is the normalized eigenvector matrix satisfying  $\mathbf{V}^T \mathbf{B} \mathbf{V} = \mathbf{I}$ , and

$$\mathbf{V}^T \mathbf{A} \mathbf{V} = \boldsymbol{\Lambda} = \text{diag}(\lambda_1, \lambda_2, \dots, \lambda_{2N})$$

in (2.7) leads to the uncoupled modal equations for the complex-valued functions  $\mathbf{z}(t)$  with generalized forcing function  $\mathbf{r} = \mathbf{V}^T \mathbf{R}$  given by

$$\dot{\mathbf{z}}(t) + \mathbf{\Lambda} \mathbf{z}(t) = \mathbf{r}(t) \quad (2.9)$$

$$\mathbf{z}(0) = \mathbf{V}^T \mathbf{B} \mathbf{y}(0) \quad (2.10)$$

or for each complex-valued mode  $k = 1, 2, \dots, 2N$

$$z'_k(t) + \lambda_k z_k(t) = r_k(t), \quad z_k(0) = \mathbf{V}_k^T \mathbf{B} \mathbf{y}_0 \quad (2.11)$$

### Update Formulas for Modal Solutions

Consider a partition of the time domain into discrete points  $0 = t_1 < t_2 < \dots < t_{ns+1} = t_f$ . The time-step is defined by  $h = t_{n+1} - t_n$  where  $t_n$  is the time at the beginning of a current step. It is of interest to solve first-order differential equations of type (2.11) for complex-valued scalar functions  $z_k(t)$  or equivalently  $g_k(t)$  in (2.6) step-by-step in time, i.e. to solve complex-valued functions of the form

$$z'(t) + \lambda z(t) = r(t), \quad (2.12)$$

with initial condition  $z(t_n) = z_n$  known at the beginning of a time step, starting from  $t_1 = 0$ . It is assumed that loading data  $\mathbf{F}(t_n)$  is given at discrete time steps, thus  $r(t)$ , for each  $k$  is known at all time-steps. An explicit solution to (2.12) is obtained by first multiplying through by  $e^{\lambda t}$ . The result can be written  $(ze^{\lambda t})' = re^{\lambda t}$ . Integrating and evaluating the initial condition  $z(t_n) = z_n$  leads to the general solution for  $t > t_n$

$$z(t) = \int_{t_n}^t r(s) e^{-\lambda(t-s)} ds + z_n e^{-\lambda(t-t_n)} \quad (2.13)$$

The integral term is recognized as the particular solution for nonhomogeneous loading, while the second-term is the complementary homogeneous solution for the initial condition at the beginning of the time step. This solution can also be derived indirectly using the Laplace transform [13]. Approximating the force  $r(t) \approx r(t_n)$  by a

constant within a time-step  $t_n < t < t_{n+1} = t_n + h$ , and evaluating (2.13) at  $t = t_{n+1}$ , the solutions for each complex mode  $k = 1, 2, \dots$ , at the next step  $z_{n+1}^k = z_k(t_{n+1})$  may be determined by the well-known update formula [14]:

$$z_{n+1}^k = r_k(t_n) \int_{t_n}^{t_{n+1}} e^{-\lambda_k(t_{n+1}-s)} ds = W_0^k r_k(t_n) + z_n^k e^{-\lambda_k h} \quad (2.14)$$

where  $W_0^k = (1 - e^{-\lambda_k h})/\lambda_k$ .

For high-order accuracy, general piecewise polynomial interpolation of order  $p$  is introduced for the loading and the forcing function over a time interval is approximated as

$$r(t) \approx \sum_{i=1}^{p+1} L_i(t) r_i \quad (2.15)$$

where  $r_1 = r(t_n), r_2 = r(t_{n+1})$ , etc. are forcing functions evaluated at discrete points and  $L_i(t)$  are Lagrangian interpolation functions

$$L_i(t) = \prod_{\substack{j=1 \\ j \neq i}}^{p+1} \frac{(t - t_j)}{(t_i - t_j)}$$

Linear interpolation corresponds to  $p = 1$ ; quadratic interpolation corresponds to  $p = 2$ , etc. Introducing the polynomial interpolation of order  $p$  for the forcing function gives the interpolatory quadrature formula

$$\begin{aligned} z(t) &= \int_{t_n}^t \sum_{i=1}^{p+1} L_i(s) r_i e^{-\lambda(t-s)} ds + z_n e^{-\lambda(t-t_n)} \\ &= \sum_{i=1}^{p+1} r_i W_i + z_n e^{-\lambda(t-t_n)} \end{aligned} \quad (2.16)$$

with weights

$$W_i(t) = \int_{t_n}^t L_i(s) e^{-\lambda(t-s)} ds \quad (2.17)$$

Expressing the Lagrangian interpolation functions as polynomials defined in time variable  $s$ , the quadrature weights can be written in terms of polynomial coefficients as shown.

$$L_i(s) = \sum_{j=0}^p C_j s^j$$

$$W_i(t) = \sum_{j=0}^p C_j \int_{t_n}^t s^j e^{-\lambda(t-s)} ds = \sum_{j=0}^p C_j I_j(t) \quad (2.18)$$

where

$$I_j(t) = \int_{t_n}^t s^j e^{-\lambda(t-s)}$$

The quadrature rule provides a time-stepping method which is driven by the initial solution  $z_n = z(t_n)$  at the beginning of the current step and advanced to the next step  $z_{n+1} = z(t_{n+1})$  by simple evaluations. Using polynomial interpolation of the forcing function, the time integral in (2.13) is recognized as a weighted integral with a complex exponential weighting function  $w(t) = e^{\lambda t}$ . The quadrature weights are evaluated in closed-form by evaluating integrands of polynomials multiplied by the exponential, i.e.

$$\int s^j e^{\lambda s} ds = \frac{1}{\lambda} s^j e^{\lambda s} - \frac{j}{\lambda} \int s^{j-1} e^{\lambda s} ds$$

For linear interpolation of the generalized forcing functions  $r_k(t)$  within a time-step  $t_n < t < t_{n+1}$ ,  $p = 1$  and the coefficients of Lagrangian interpolation polynomial and integrals defined in (2.18) are

$$C_0 = \frac{(-1)^{i-1}}{h} t_{(n+2)-i}$$

$$C_1 = \frac{(-1)^i}{h}$$

$$I_0 = \frac{1}{\lambda_k} [1 - e^{-\lambda_k h}],$$

$$I_1 = \frac{1}{\lambda_k^2} [(\lambda_k t_{n+1} - 1) - (\lambda_k t_n - 1)e^{-\lambda_k h}]$$

Evaluating (2.16) at  $t = t_{n+1}$  the complex mode solutions at the next step are given by the update formula

$$z_{n+1}^k = W_1^k r_k(t_n) + W_2^k r_k(t_{n+1}) + z_n^k e^{-\lambda_k h} \quad (2.19)$$

with quadrature weights for complex mode  $k$

$$W_1^k = \frac{1}{\lambda_k} \left( \frac{1}{\lambda_k h} - e^{-\lambda_k h} \left( 1 + \frac{1}{\lambda_k h} \right) \right),$$

$$W_2^k = \frac{1}{\lambda_k} \left( 1 - \frac{1}{\lambda_k h} (1 - e^{-\lambda_k h}) \right).$$

This result matches the closed-form algorithm previously derived by Dickens [15] where piecewise linear loading was assumed for  $r_k(t)$  and the solution to (2.11) was obtained by summing the general homogeneous solution  $z_k(t) = A_k e^{-\lambda_k t}$ , with assumed particular solutions of the form of a linear polynomial  $z_k(t) = B_k + C_k t$  and matching coefficients. The algorithm is exact for solutions driven with piecewise linear forcing functions and initial conditions. Detailed derivation of exact solution using linear interpolation of forcing functions and matching of results obtained by Dickens [15] is provided in the Appendix.

To derive an algorithm which is exact for solutions driven by piecewise quadratic forcing functions and initial conditions, quadratic interpolation of  $r_k(t)$  is used within a time-interval  $t_n < t < t_{n+2} = t_n + 2h$  with equally spaced time step  $h \rightarrow h_n$ , in (2.16) and evaluate  $t = t_{n+2}$ . The coefficients of Lagrangian interpolation polynomial

and integrals defined in (2.18) are

$$\begin{aligned}
C_0 &= \frac{(-1)^{i-1}}{h^2} \left(\frac{1}{2}\right)^{(i-2)^2} \prod_{\substack{m=0 \\ m+1 \neq i}}^{p+1} t_{(n+m)}, \\
C_1 &= \frac{(-1)^i}{h^2} \left(\frac{1}{2}\right)^{(i-2)^2} \sum_{\substack{m=0 \\ m+1 \neq i}}^{p+1} t_{(n+m)}, \\
C_2 &= \frac{(-1)^{i-1}}{h^2} \left(\frac{1}{2}\right)^{(i-2)^2} \\
I_0 &= \frac{1}{\lambda_k} [1 - e^{-2\lambda_k h}], \\
I_1 &= \frac{1}{\lambda_k^2} [(\lambda_k t_{n+2} - 1) - (\lambda_k t_n - 1)e^{-2\lambda_k h}], \\
I_2 &= \frac{1}{\lambda_k^3} [(\lambda_k t_{n+2}^2 - 2\lambda_k t_{n+2}) - (\lambda_k t_n^2 - 2\lambda_k t_n + 2)e^{-2\lambda_k h}],
\end{aligned}$$

with the result

$$z_{n+2}^k = W_1^k r_k(t_n) + W_2^k r_k(t_{n+1}) + W_3^k r_k(t_{n+2}) + z_n^k e^{-2\lambda_k h} \quad (2.20)$$

and quadrature weights

$$\begin{aligned}
W_1^k &= -\frac{1}{2\lambda_k(\beta_k)^2} ((2(\beta_k)^2 + 3\beta_k + 2)e^{-2\beta_k} + (\beta_k - 2)), \\
W_2^k &= \frac{2}{\lambda_k(\beta_k)^2} ((\beta_k + 1)e^{-2\beta_k} + (\beta_k - 1)), \\
W_3^k &= \frac{1}{2\lambda_k(\beta_k)^2} ((2(\beta_k)^2 - 3\beta_k + 2) - (\beta_k + 2)e^{-2\beta_k}),
\end{aligned}$$

where  $\beta_k = \lambda_k h$ . The above algorithm assumes that the loading data is known at discrete data points only. If the loading  $\mathbf{F}(t)$  is a continuous function in time, then the algorithm above can be modified to evaluate the forcing function at  $r_k(\frac{t_n+t_{n+1}}{2})$  and the solution advanced to  $z_{n+1}$ . For cubic ( $p = 3$ ) and higher order update formulas can be easily obtained from (2.16)-(2.18).

For comparison, Trapezoidal and Simpson quadrature rules are also considered based on linear and quadratic interpolation of the entire integrand in (2.13) with unit

weight

$$f(s) = r(s) e^{-\lambda(t-s)} \approx \sum_{i=1}^{p+1} L_i(s) f_i \quad (2.21)$$

where  $f_1 = f(t_n)$ ,  $f_2 = f(t_{n+1})$ , etc. For trapezoidal rule, evaluating (2.13) at  $t = t_{n+1}$ , the resulting algorithm is

$$\begin{aligned} z_{n+1}^k &= \frac{h}{2} (f_k(t_n) + f_k(t_{n+1})) + z_n^k e^{-\lambda_k h} \\ &= W_1^k r_k(t_n) + W_2^k r_k(t_{n+1}) + z_n^k e^{-\lambda_k h} \end{aligned} \quad (2.22)$$

with quadrature weights

$$W_1^k = \frac{h}{2} e^{-\lambda_k h}, \quad W_2^k = \frac{h}{2}$$

For Simpson's  $\frac{1}{3}$  rule, evaluating (2.13) at  $t = t_{n+2}$ , with  $f(s)$  approximated by a quadratic polynomial interpolation of order  $p = 2$ , the resulting algorithm is

$$\begin{aligned} z_{n+2}^k &= \frac{h}{3} (f_k(t_n) + 4f_k(t_{n+1}) + f_k(t_{n+2})) + z_n^k e^{-2\lambda_k h} \\ &= W_1^k r_k(t_n) + W_2^k r_k(t_{n+1}) + W_3^k r_k(t_{n+2}) + z_n^k e^{-2\lambda_k h} \end{aligned} \quad (2.23)$$

and quadrature weights

$$W_1^k = \frac{h}{3} e^{-2\lambda_k h}, \quad W_2^k = \frac{4h}{3} e^{-\lambda_k h}, \quad W_3^k = \frac{h}{3}$$

In the above, it is assumed that the loading is known only at discrete uniformly spaced data points. If the loading  $\mathbf{F}(t)$  is a continuous function in time, then high-order quadrature rules such as Gauss-Legendre can also be used. For the case of uncoupled real modes with proportional damping, update formulas based on numerical approximation of Duhamel's integral with Trapezoidal and Simpson rules are derived in [21].

The complex valued modal solution is obtained step-by-step from the update formulas starting from the initial condition until the final time of interest is reached. For constant time-step size  $h$ , the weights  $W_i^k$  may be calculated and stored for each

complex mode prior to the time-step loop to reduce the number of evaluations. For the eigenvalues which occur as complex numbers, the eigenvalues and eigenvectors occur in conjugate pairs, and the corresponding modal solutions occur in complex conjugate pairs. Additional savings can be achieved by solving the time-history for only one of the modes in the conjugate pair and performing the summation in the transformation  $\mathbf{y}(t) = \mathbf{V}\mathbf{z}(t)$  with real values only [13, 15].

$$\mathbf{y}(t) = \mathbf{V}\mathbf{z}(t) = \sum_{i=1,3,\dots,2N-1} 2 (\mathbf{V}_i^R \mathbf{z}_i^R - \mathbf{V}_i^I \mathbf{z}_i^I) \quad (2.24)$$

The state-space modal method is computationally efficient with limited memory or disk requirements once the complex eigensolution of size  $2N_r$  is amortized over time-steps.

Physical space counter-parts of the constant and linear force modal update formulas (2.14) and (2.19) involve direct discrete-transition matrices in terms of the matrix exponential  $e^{-\tilde{\mathbf{A}}h}$  [17, 14], obtained by solving the state-space equation

$$\dot{\mathbf{x}}(t) = \tilde{\mathbf{A}}\mathbf{x}(t) + \tilde{\mathbf{B}}, \quad \mathbf{x}(t) = [\mathbf{u}(t); \mathbf{v}(t)]$$

where

$$\tilde{\mathbf{A}} = \begin{bmatrix} \mathbf{0} & \mathbf{I} \\ -\mathbf{M}^{-1}\mathbf{K} & -\mathbf{M}^{-1}\mathbf{C} \end{bmatrix}, \quad \tilde{\mathbf{B}} = \begin{Bmatrix} \mathbf{0} \\ \mathbf{M}^{-1}\mathbf{F}(t) \end{Bmatrix}, \quad \mathbf{x}(0) = [\mathbf{u}_0; \mathbf{v}_0].$$

with the exact solution from convolution integral

$$\mathbf{x}(t) = e^{\tilde{\mathbf{A}}(t-t_0)}\mathbf{z}(t_0) + e^{\tilde{\mathbf{A}}t} \int_{t_0}^t e^{-\tilde{\mathbf{A}}s} \mathbf{F}(s), ds$$

This alternative discrete-time transition approach requires evaluation of  $e^{\tilde{\mathbf{A}}h}$  usually obtained by a direct Taylor-series expansion with scaling used to speed convergence [18]. Direct discrete-time transition matrix counter-parts of the Trapezoid and Simpson's rule update formulas (2.22), (2.23) and our quadratic force interpolation



update formula (2.20) can also be easily obtained. The cost of solving the complex eigenvalue problem in the modal approach advocated here is balanced by the significantly smaller effort required to compute the quadrature weights  $W_i^k$  in the modal update formulas than to directly compute  $e^{\tilde{\mathbf{A}}h}$ . Another advantage of the modal analysis approach is that any spurious modes from spatially discrete approximations of continuous systems can be removed in a reduced real modal solution prior to obtaining state-space modal solutions without need for filtering of the post-processed solution required in the direct discrete-time transition matrix approach.

The algorithm for obtaining the update formulas using single-step complex eigen analysis method is summarized below:

1. Solve complex eigenvalue problem  $(\mathbf{A} - \lambda_k \mathbf{I})\mathbf{V}_k = 0$  for  $\lambda_k$  and  $\mathbf{V}_k$ , where  $\mathbf{A}$  is defined in (2.8).
2. Form initial conditions  $z_k(0) = \mathbf{V}_k^T \mathbf{B} \mathbf{y}_0$  for each mode and generalized force  $r = \mathbf{V}^T \mathbf{R}$ .
3. For each complex conjugate pair, calculate weights  $W_i^k$  for solution update formulas.
4. Loop over time-steps with size  $h$  to advance the solution from current to next time step. For each complex conjugate pair, solution can be obtained by summation of real values only as given in (2.24). Update formulas depend on order of approximation assumed for forcing function. See (2.19) and (2.20) for linear and quadratic approximations respectively.
5. Transform the solution back to physical coordinates using  $y(t) = \mathbf{V}z(t)$ .

Alternatively, the two-step modal analysis involving real eigenvalue problem retaining certain number of modes followed by complex eigen problem can be employed if it is required to eliminate any spurious mode present in the system. The algorithm for the two-step analysis is as follows:

1. Solve the real eigenvalue problem  $(\mathbf{K} - \omega_i^2 \mathbf{M})\boldsymbol{\varphi}_i = \mathbf{0}$  for  $\omega_i$  and  $\boldsymbol{\varphi}_i$ , where  $\mathbf{K}$  and  $\mathbf{M}$  are defined in (1.1).
2. Use modal transformation with  $N_r$  retained modes  $\mathbf{u}(t) = \mathbf{P}_r \mathbf{q}_r(t)$  to reduce the coupled dynamic system equation to modal differential equations given in (2.2).
3. Solve complex eigenvalue problem  $(\hat{\mathbf{K}} - \hat{\lambda}_k \mathbf{I})\boldsymbol{\psi}_k = 0$  for  $\lambda_k$  and  $\boldsymbol{\psi}_k$ , where  $\hat{\mathbf{K}}$  is defined in (2.4).
4. Form initial conditions  $g_k(0) = \boldsymbol{\Psi}_k^T \hat{\mathbf{M}} \mathbf{x}_0$  for each mode and generalized force  $G = \boldsymbol{\Psi}^T \hat{\mathbf{Q}}$ .
5. Repeat steps 3 to 5 from single-step modal analysis.

A variable time step  $h_n$  could be used with no difficulty. The only change would be the weights ( $W_i^k$ ) need to be recomputed at each time step.

CHAPTER 3  
NUMERICAL EXAMPLES

An example problem for comparing the results obtained using the different interpolation methods with non-proportional viscous damping is shown in Figure 3.1. The physical setup is comprised of two lumped masses connected in series by three linear springs, two dampers and restrained at the ends. The coupled equations of motion for this system are

$$\begin{bmatrix} m_1 & 0 \\ 0 & m_2 \end{bmatrix} \begin{Bmatrix} \ddot{u}_1(t) \\ \ddot{u}_2(t) \end{Bmatrix} + \begin{bmatrix} c_1 + c_2 & -c_2 \\ -c_2 & c_2 \end{bmatrix} \begin{Bmatrix} \dot{u}_1(t) \\ \dot{u}_2(t) \end{Bmatrix} + \begin{bmatrix} k_1 + k_2 & -k_2 \\ -k_2 & k_2 + k_3 \end{bmatrix} \begin{Bmatrix} u_1(t) \\ u_2(t) \end{Bmatrix} = \begin{Bmatrix} F_1(t) \\ F_2(t) \end{Bmatrix}$$

where  $u_1(t)$  and  $u_2(t)$  are displacements and  $F_1(t), F_2(t)$  are loading functions at the lumped masses. The mass and stiffness parameters are set to  $m_1 = m_2 = 1$ , and

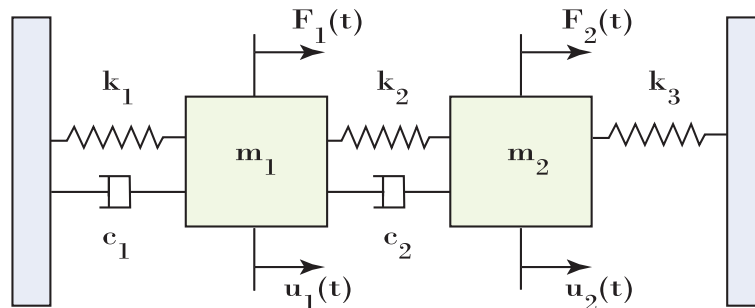


Figure 3.1: Numerical example with non-proportional damping setup.

$k_1 = k_2 = k_3 = 4\pi^2$ , such that the system is tuned to have undamped natural frequencies of  $f_1 = 1$  Hz and  $f_2 = \sqrt{3}$  Hz. The masses are driven by equal and opposite sinusoidal forcing functions with amplitude 10 and frequency of  $f = 1.5$  Hz, i.e.

$$\begin{pmatrix} F_1(t) \\ F_2(t) \end{pmatrix} = \begin{pmatrix} 10 \sin(3\pi t) \\ -10 \sin(3\pi t) \end{pmatrix}$$

The non-proportional damping parameters are set to  $c_1 = c_2$  and  $c_3 = 0$ . Two damping cases considered are  $c_1 = c_2 = (4\pi)/50$  and  $c_1 = c_2 = 4\pi$  corresponding to light and very heavy damping, respectively. The modal damping ratios obtained by modal transformation neglecting damping, and neglecting off-diagonal modal damping in the pseudo-uncoupled equations correspond to  $\zeta_1 = 0.01(1\%)$  and  $\zeta_2 = 0.0289(2.89\%)$  for light damping, and  $\zeta_1 = 0.5(50\%)$  and  $\zeta_2 = 1.4434$  (super-critically damped).

Results obtained using the weighted linear and quadratic polynomial interpolation of the forcing function and update formulas (2.19) and (2.20) will be denoted P1 and P2, respectively, and compared to piecewise constant (P0) and Trapezoidal and Simpson's quadrature rules for integrating the particular solution. The time-step size  $h = t_{n+1} - t_n$  is set to a fixed value  $T/h = 20$  corresponding to 20 increments per driving period  $T = 1/1.5$  sec. Initial conditions are set to zero.

Figure 3.2 shows the displacements of Mass-1 and Mass-2 for the light damping case comparing P0 and P1. The response with the piecewise constant load approximation (P0) shows significant error in the solution while the results for P1 shows a small error associated with the linear approximation of the forcing term. These observations are examined further in Figure 3.3, which shows the error in displacement for Mass-1. These results show that in the light damping case considered, the error for P0 is the highest and the accuracy of the Trapezoidal integration method is

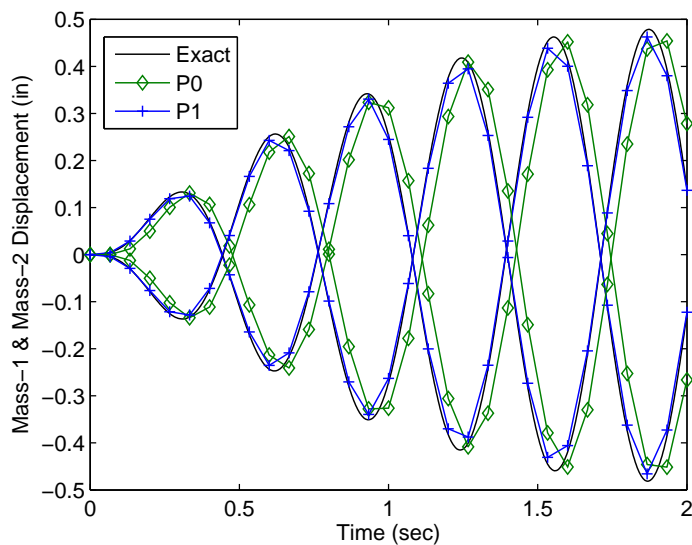


Figure 3.2: Displacements for Mass-1 and Mass-2 with non-proportional light damping, comparing piecewise constant (P0) and linear (P1) load approximations to exact solutions.

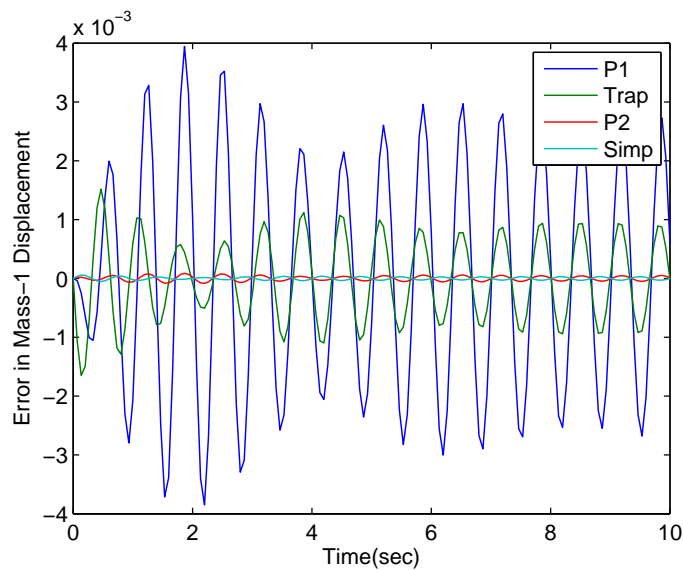


Figure 3.3: Error in Displacements for Mass-1 with light damping. Error in displacement for P0 is between  $10^{-2}$  and  $10^{-1}$  (not shown).

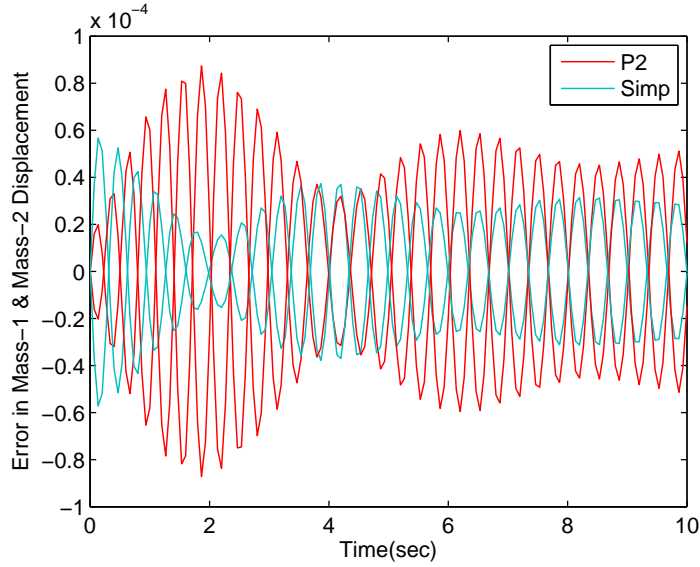


Figure 3.4: Error in Displacements for Mass-1 and Mass-2 and light damping comparing piecewise quadratic load approximation (P2) and Simpson’s rule.

slightly more accurate than the linear force approximation method P1. As expected the accuracy of the higher-order Simpson’s integration and P2 methods are improved. A similar result is found for Mass-2. Figure 3.4 shows that for the case of light damping considered, Simpson’s method is slightly more accurate than P2. The P0 update formulas result in a large error in displacement.

Figure 3.5 shows the displacements of Mass-1 and Mass-2 for the very heavy damping case, comparing P0 and P1 methods with the exact solution. The error in displacement for Mass-1 is shown in Figure 3.6. The results show that P0 has the largest error, and for the Trapezoidal and Simpson’s method the difference in error between the light damping and heavy damping cases remains relatively unchanged. In contrast, for the very heavy damping case, the error is significantly reduced for the P1 and P2 methods compared to the light damping case. As a result of the reduction of error with increased damping, for the heavy damping considered, P1

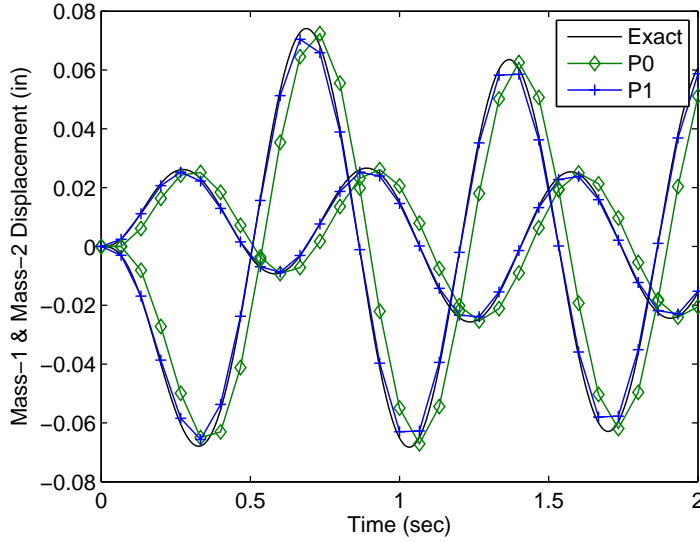


Figure 3.5: Displacements for Mass-1 and Mass-2 with very heavy non-proportional damping, comparing piecewise constant (P0) and linear (P1) load approximations to exact solutions.

and P2 are significantly more accurate than Trapezoidal and Simpson, respectively. The influence of damping on the error is illustrated in Fig. 3.7 where the response error is shown with the non-proportional damping value changing between  $0 \leq c \leq 4\pi$ . A similar result was found for Mass-2 and other proportional and non-proportional damping distributions. In all cases considered, there is a large reduction in error for P1 compared to P0, however, the improvement in accuracy in moving from P1 to P2 is not as significant.

In the absence of any load applied to the system, the general solution in complex domain defined in 2.13 reduces to the homogeneous part  $z_n e^{-\lambda(t-t_n)}$  depending explicitly on the time step size  $h$  and the complex eigen mode  $\lambda_h$ . The numerical example system model was driven with initial conditions  $\mathbf{u}_0 = [1; -1]$  and  $\mathbf{v}_0 = [0; 0]$  and no loading and a plot comparing the exact and P1 methods for low damping scenario is shown in Fig. 3.9 indicating that the solutions for P1 and exact methods

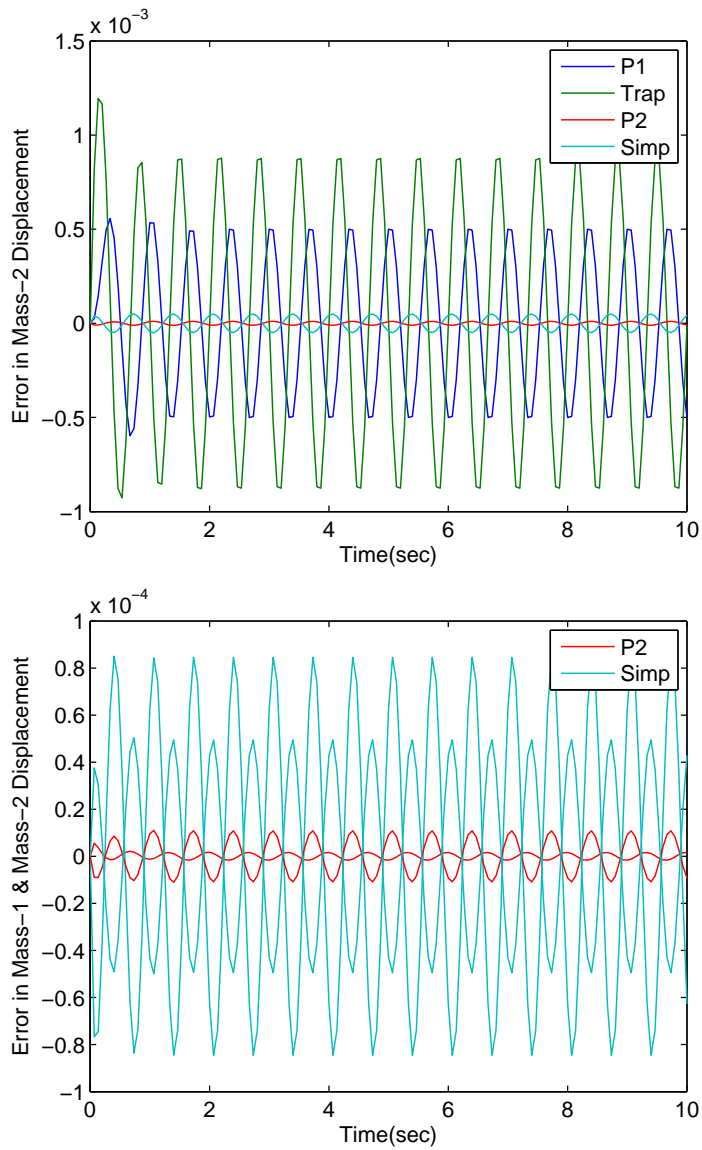


Figure 3.6: Error in Displacements with very heavy non-proportional damping: (Top) Comparing all methods, (Bottom) Comparing P2 and Simpson only. Error in displacement for P0 is approximately  $10^{-2}$  (not shown).



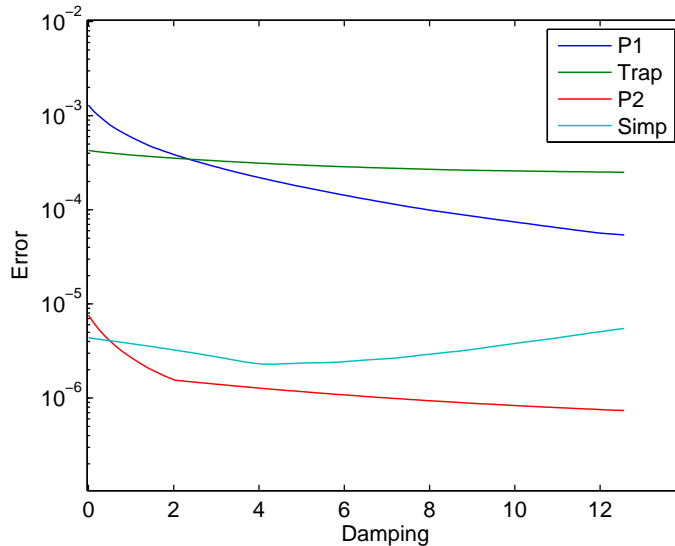


Figure 3.7: Error versus non-proportional damping measured by  $0 \leq c \leq 4\pi$ .

overlap or match each other. Similar results were obtained for other interpolation methods.

### Convergence Rates

Local truncation error for interpolatory quadrature rules are proportional to step size  $h = t_{n+1} - t_n$ , the weight function  $w(t)$  in the time-step integral, and on the maximum of the  $d + 1$  continuous derivative of the function interpolated over the step, where  $d$  is the highest polynomial exactly integrated [22]. For Trapezoidal and Simpson's rule, the weight  $w \equiv 1$ , so that the local error from numerical integration of  $z(t)$  over a step of size  $h$  is  $|E| \leq C h^{d+2}$ , where  $d = 1$  and  $d = 3$ , respectively. The sum of the local truncation error over all time-steps is one-order less than the local error. Thus the convergence rate of solutions from time-step size reduction expected by Trapezoidal and Simpson's rules are order  $O(h^2)$  and  $O(h^4)$ , respectively. The situation is more involved for the load interpolation methods, where the forcing

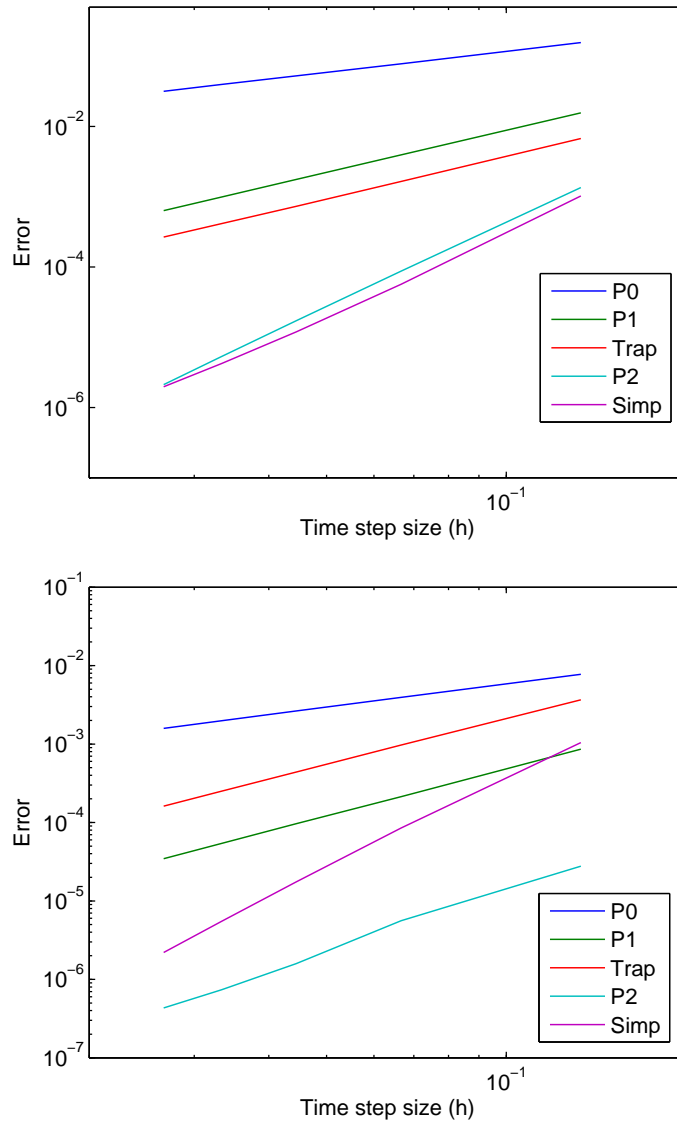


Figure 3.8: Error versus time-step size for Mass-1, (a) light damping, (b) very heavy damping

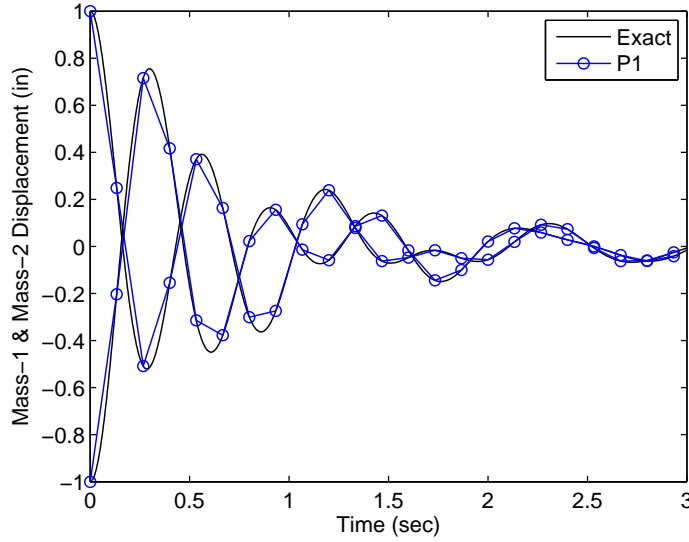


Figure 3.9: Displacements for Mass-1 and Mass-2 comparing P1 method with Exact solution subject to initial conditions for light damping

function  $r(t)$  in the exact solution integral (2.13) is interpolated with a weight function  $w(t) = e^{\lambda t}$ . In this case, the local error depends explicitly on the amount of damping relative to the step size as measured by  $\lambda_k h$ .

Figure 3.8 shows the plots of error in displacement for Mass-1 versus time step size  $h$  in log scale for light and very heavy damping cases. The convergence rates of the methods are indicated by the slope of the curve on the log-log plot. The convergence rate found for P0 is  $O(h)^1$ . For methods P1 and Trapezoidal the convergence rate is found to be relatively invariant with damping, showing a convergence rate of order two with time-step size,  $O(h)^2$ . Simpson's rule shows a convergence rate of order four,  $O(h)^4$  as expected from error estimates. A significant reduction in convergence rate with very heavy damping is seen for the P2 method changing from  $O(h)^4$  for light damping to  $O(h)^3$  for very heavy damping. In the limit of no damping, the eigenvalues  $\lambda_k$  are purely imaginary, and P2 shows the same convergence rate as Simpson's rule.

While not shown in the plots, in the limit of super-critical damping for all modes, the eigenvalues  $\lambda_k$  are purely real and P2 showed a reduced convergence rate of approximately  $O(h)^2$ , yet overall, P2 exhibits significantly reduced error compared to Simpson's rule for heavy damping. Similar results were found for Mass-2 and other damping cases including proportional damping. Overall, for systems with continuous forcing input and light damping, standard Trapezoidal and Simpson's rule integration exhibit slightly improved accuracy. For systems with heavy damping, the weighted force interpolation quadrature rules are more accurate.

### Spurious Mode Reduction

For direct time integration methods which do not utilize modal information, such as the HHT- $\alpha$  [19] method used in many commercial finite element codes, the property of asymptotic mode annihilation is desirable to reject or dissipate any spurious modes resulting from spatial discretization of a continuous physical system [1]. The problem of spurious mode rejection is a characteristic of 'stiff systems'. A deficiency of the direct discrete-time transition methods [14] is the lack of asymptotic mode annihilating capability since these methods simply emulate the behavior of the spatially discrete equations. In an attempt to reject spurious high frequency modes in solutions using the linear force discrete-time transition method developed in [17], discrete-time filtering algorithms have been employed which are not entirely effective in eliminating the spurious high-frequency response [23]. The advantage of the modal approach advocated here is that a two-step process can be taken; first a real-valued undamped modal reduction is performed using (2.1) and (2.2) by eliminating the spurious modes and retaining only the  $N_r \leq N$  physical modes; then the reduced real-valued modal equations can be cast in state-space form (2.4) and uncoupled using complex modal analysis in (2.6) with the state-space modal solutions obtained

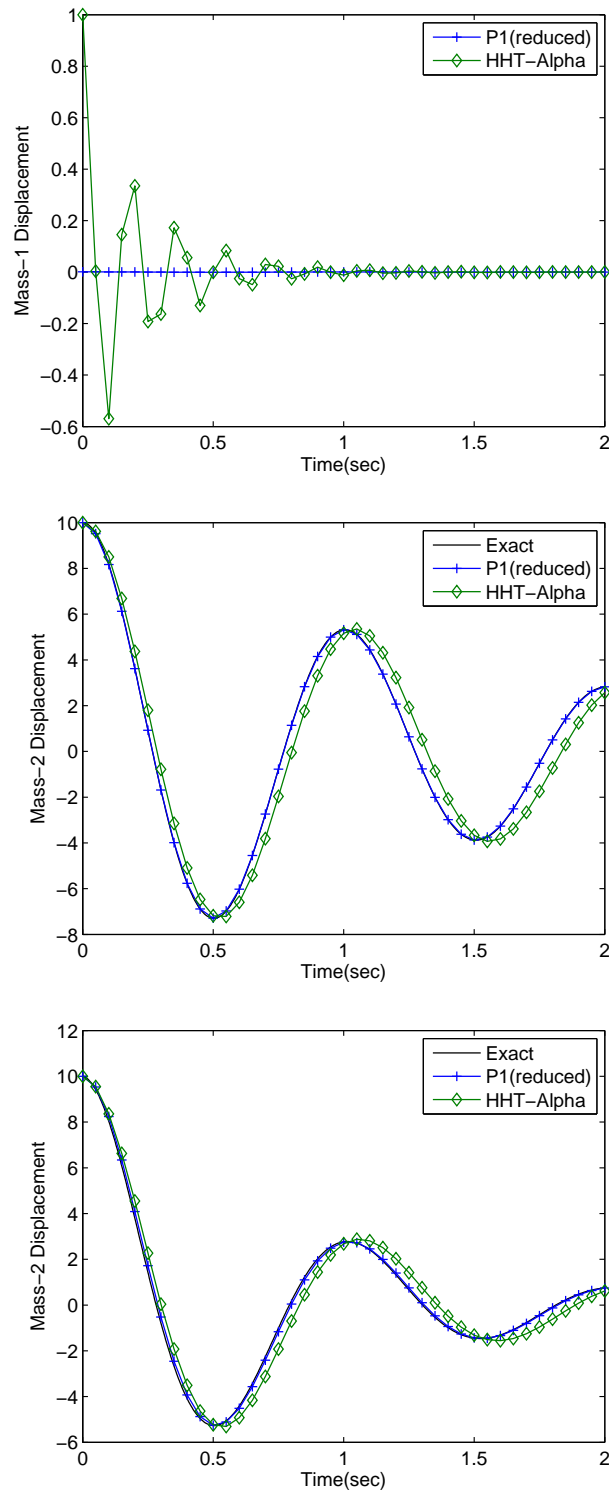


Figure 3.10: (Top): Mass-1 displacement for proportional and non-proportional damping. (Middle): Mass-2 displacement for proportional damping and (Bottom): Mass-2 displacement for non-proportional damping

efficiently using any one of the step-by-step update formulas derived in (2.19) or (2.20).

The spurious mode rejection capability of the modal reduction approach is illustrated and compared to the damped HHT- $\alpha$  [19] time-integration method ( $\alpha = -0.3$ ) using an extension of a second-order undamped system considered in [1] generalized with proportional and non-proportional damping, where the system is defined by

$$\mathbf{M}\ddot{\mathbf{u}}(t) + \mathbf{C}\dot{\mathbf{u}}(t) + \mathbf{K}\mathbf{u}(t) = 0$$

$$\mathbf{M} = \begin{bmatrix} \mathbf{m}_1 & \mathbf{0} \\ \mathbf{0} & \mathbf{m}_2 \end{bmatrix}, \mathbf{K} = \begin{bmatrix} \mathbf{k}_1 + \mathbf{k}_2 & -\mathbf{k}_2 \\ -\mathbf{k}_2 & \mathbf{k}_2 \end{bmatrix}$$

It is assumed  $k_1 = (10^4) k_2$ , where  $k_2 = 4\pi^2$  and  $m_1 = m_2 = 1$  to represent the character of a typical large system. The first mode ( $f_1 \sim 1$  Hz) is intended to represent the modes that are physically important and must be accurately integrated. The second mode ( $f_2 \sim 100$  Hz) represents the spurious high frequency modes. The initial conditions are  $\mathbf{u}_0 = [1; 10]$  and  $\mathbf{v}_0 = [0; 0]$ . Values for structural damping typically correspond to modal damping ratios  $\zeta \leq 20\%$ .

Using a time-step size of  $T_1/h = 20$ , the response of the damped HHT- $\alpha$  method ( $\alpha = -0.3$ ) is compared to a modal analysis which retains only the first real-valued mode and solves the reduced modal equations with the complex state-space modal analysis and update formulas. Results for two damping cases are shown in Figure 3.10 for mass-proportional damping with  $\mathbf{C} = \text{diag}[c; c]$  where  $c = 4\pi/10$  corresponding to a modal damping ratio  $\zeta_1 = 10\%$ , and non-proportional damping with  $\mathbf{C} = [2c, -c; -c, c]$  where  $c = 4\pi/5$  corresponding to a proportional modal damping ratio  $\zeta_1 = 20\%$ . In both cases, the modal damping ratio for the high spurious mode is less than 0.4%. The exact response with no modal reduction produces a

solution for Mass-1 with high-frequency oscillations of  $\sim 100$  Hz which are intended to be eliminated. For both the proportional and non-proportional damping cases, the reduced modal analysis approach, denoted P1 (reduced), effectively eliminates the response of Mass-1 while maintaining the high accuracy of the Mass-2 response. In contrast, the HHT- $\alpha$  direct time-integration method takes several time-steps to damp out the Mass-1 response while adversely effecting the accuracy of the Mass-2 response. Similar results were obtained for smaller damping ratios.

## CHAPTER 4

### CONCLUSIONS

The complex modal analysis method for coupled damping time history response proposed by Dickens [15] is evaluated and compared to alternatives for approximating the time integral of the weighted forcing function in the exact solution to state-space modal equations. The time integral of the forcing function is recognized as a weighted integral with a complex exponential and using polynomial interpolation for the forcing function, derive general update formulas. Closed-form expressions are derived for piecewise linear and quadratic force interpolations over time-steps. Linear approximation for loading within a time-step used by Dickens is shown to be a special case of the quadrature rules with linear interpolation. The solution methods are exact for piecewise linear and quadratic loading with or without initial conditions and are computationally efficient with low memory for time-history response of linear dynamic systems including general non-proportional viscous damping. It is shown that local error for interpolatory quadrature depends explicitly on the amount of damping relative to the step size as measured by  $\lambda_k h$ .

Numerical results for an example system with general, non-proportional damping and driven with a continuous forcing function shows the improved accuracy of the linear and quadratic interpolations compared to well-known piecewise constant load approximation. The convergence for the linear force interpolation method is found to be relatively invariant with damping, showing a convergence rate of order two with time-step size. In the limit of no damping, the eigenvalues of the modal state-space equations are purely imaginary, and the quadratic force interpolation method showed the same 4th-order convergence rate as Simpson's rule. In the limit of super-critical damping for all modes, the state-space eigenvalues are purely real and the



quadratic force interpolation method showed a reduced convergence rate of approximately two, yet overall, exhibited significantly reduced error compared to Simpson's rule for heavy damping. Overall, for systems with continuous forcing input and light damping, standard Trapezoidal and Simpson's rule integration gave comparable accuracy to piecewise linear and quadratic force approximations. For systems with heavy damping, the weighted force interpolation quadrature rules showed improved accuracy. Using a simple model developed in [1], a two-step modal analysis using real-valued modal reduction followed by state-space modal analysis is shown to be an effective approach for rejecting any spurious modes occurring in stiff systems with general damping arising from spatial discretization of continuous physical systems.

In summary, contributions include recognizing a systematic framework for deriving high-order polynomial interpolatory quadrature rules for integration of the exact complex modal solutions; deriving exact closed form quadrature weights for linear and quadratic force interpolation; recognizing that local error depends explicitly on the amount of damping in the system as measured by the complex eigenvalues of the state-space modal equations; showing the relative accuracy of the different quadrature methods for continuous force input with varying degrees of non-proportional damping, and demonstrating the effectiveness of a two-step modal analysis in eliminating spurious modes in stiff systems with general damping by first performing an undamped modal reduction, then performing a state-space modal analysis and retaining only physical modes.

### Future Work

Having determined the exact solution for general non-proportionally damped dynamic systems for piece-wise linear and quadratic loading, there remain areas for further development that would help utilize the ideas presented to their full potential. Below are the key avenues identified for future work:

- Extend the scope of numerical examples to incorporate solutions obtained by moving the cross-coupling terms from damping matrix to right-hand-side as a pseudo-loading term [5, 11] and evaluating the solution by iterative techniques in order to make a comparison with the solution proposed by Dickens [15].
- Study Direct Discrete-time transition matrix solution for general dynamic systems [17, 14] which requires evaluation of the exponential state-space matrix obtained by direct Taylor-series expansion with scaling used to speed convergence [18] to compare the computational efficiency with the exact solution obtained using complex mode superposition.
- By utilizing indices measuring the non-proportionality of dynamic systems proposed by [9, 10], the two-step modal analysis using real-valued modal reduction followed by state-space modal analysis techniques can be analyzed in detail to quantify the effect of modal reduction on the amount of non-proportionality existing in the system studied.
- Derive expressions for error estimates corresponding to linear and quadratic force interpolation methods in closed-form.

## APPENDIX

### EXACT SOLUTION FOR LINEAR INTERPOLATION FORCING FUNCTIONS

It is aimed to match the solution obtained by Dickens [15] to the exact solution obtained using complex mode superposition using linear interpolation of forcing functions.

General solution of complex valued function for each mode at time  $t_{n+1} > t_n$  is given by

$$z_k(t_{n+1}) = \int_{t_n}^{t_{n+1}} r(s)e^{-\lambda_k(t_{n+1}-s)} ds + z_n e^{-\lambda_k h} \quad (\text{A.1})$$

Introducing the polynomial of order  $p = 1$  (linear) for the forcing function gives the interpolatory quadrature formula

$$z_k(t_{n+1}) = \int_{t_n}^{t_{n+1}} [L_1(s)r(t_n) + L_2(s)r(t_{n+1})]e^{-\lambda_k(t_{n+1}-s)} ds + z_n e^{-\lambda_k h} \quad (\text{A.2})$$

$$= r(t_n)W_1 + r(t_{n+1})W_2 + z_n e^{-\lambda_k h} \quad (\text{A.3})$$

with weights

$$W_1^k = \int_{t_n}^{t_{n+1}} \left[ \frac{t_{n+1} - s}{h} \right] e^{-\lambda_k(t_{n+1}-s)} ds = \frac{1}{\lambda_k} \left( \frac{1}{\lambda_k h} - e^{-\lambda_k h} \left( 1 + \frac{1}{\lambda_k h} \right) \right)$$

$$W_2^k = \int_{t_n}^{t_{n+1}} \left[ \frac{s - t_n}{h} \right] e^{-\lambda_k(t_{n+1}-s)} ds = \frac{1}{\lambda_k} \left( 1 - \frac{1}{\lambda_k h} (1 - e^{-\lambda_k h}) \right)$$

Substituting the value of weights in the quadrature formula given in (A.2), update formulas for piece-wise linear loading is obtained.

$$z_{n+1}^k = \frac{1}{\lambda_k} \left( \frac{1}{\lambda_k h} - e^{-\lambda_k h} \left( 1 + \frac{1}{\lambda_k h} \right) \right) r_k(t_n) + \frac{1}{\lambda_k} \left( 1 - \frac{1}{\lambda_k h} (1 - e^{-\lambda_k h}) \right) r_k(t_{n+1}) + z_n^k e^{-\lambda_k h} \quad (\text{A.4})$$

An alternative method of obtaining update formula for (A.1) is to write the forcing function as  $r(t) = r_n + m(t - t_n)$ ,  $t_n \leq t \leq t_{n+1}$ , where  $m = \left( \frac{r_{n+1} - r_n}{h_n} \right)$  is the

slope.

$$z_k(t) = e^{-\lambda_k t} \int_{t_n}^t [r_n + m(s - t_n)] e^{\lambda_k s} ds + C e^{-\lambda_k t}$$

The solution is retained to be evaluated at final time  $t$  with an unknown constant of integration  $C$  as shown. Upon evaluating the integral at  $t = t_{n+1}$  with initial condition  $z(t_n) = C$ ,

$$z_k(t_{n+1}) = \left( \frac{r_n}{\lambda_k} - \frac{m}{\lambda_k^2} \right) (1 - e^{-\lambda_k h}) + \frac{m h}{\lambda_k} + z(t_n) e^{-\lambda_k h}$$

By substituting the value of slope  $m = \left( \frac{r_{n+1} - r_n}{h_n} \right)$  and simplifying, the resulting equation matches with (A.4) obtained by introducing linear polynomial approximation for the forcing function.

The solution proposed by Dickens [15] can be arrived by approximating the forcing function in the first-order differential equation in complex valued function  $z(t)$  as a linear combination of loading evaluated at current and next time step. Using normalized time  $\hat{t} = t - t_n$ ,

$$r(\hat{t}) \cong \left( 1 - \frac{\hat{t}}{h} \right) r(t_n) + \frac{\hat{t}}{h} r(t_{n+1})$$

$$\dot{z}_k(\hat{t}) + \lambda_k z_k(\hat{t}) \cong \left( 1 - \frac{\hat{t}}{h} \right) r(t_n) + \frac{\hat{t}}{h} r(t_{n+1}), \quad 0 \leq \hat{t} \leq h \quad (\text{A.5})$$

The homogeneous solution for (A.5) is given in the form  $z_k^H(\hat{t}) = A_k e^{-\lambda_k \hat{t}}$  and the particular solution is assumed of a linear form  $z_k^P(\hat{t}) = B_k + C_k \hat{t}$ . Substituting the assumed particular solution into (A.5) and matching polynomial coefficients leads to

$$B_k = \left\{ \begin{array}{cc} \frac{1}{\lambda_k} + \frac{1}{\lambda_k^2 h} & - \frac{1}{\lambda_k^2 h} \end{array} \right\} \left\{ \begin{array}{c} r_k(t_n) \\ r_k(t_{n+1}) \end{array} \right\}, \quad (\text{A.6})$$

$$C_k = \left\{ \begin{array}{cc} -\frac{1}{\lambda_k h} & \frac{1}{\lambda_k h} \end{array} \right\} \left\{ \begin{array}{c} r_k(t_n) \\ r_k(t_{n+1}) \end{array} \right\}. \quad (\text{A.7})$$

The general solution is a sum of homogeneous and particular solution,  $z_k(\hat{t}) = A_k e^{-\lambda_k \hat{t}} + B_k + C_k \hat{t}$ . Using initial condition at beginning of time step  $\hat{t} = 0$ ,  $A_k$  can be evaluated as

$$A_k = \left\{ \begin{array}{ccc} -\frac{1}{\lambda_k} - \frac{1}{\lambda_k^2 h} & -\frac{1}{\lambda_k^2 h} & 1 \end{array} \right\} \left\{ \begin{array}{c} r_k(t_n) \\ r_k(t_{n+1}) \\ z_k(t_n) \end{array} \right\}, \quad (\text{A.8})$$

At  $t_{n+1}$ , the general solution can be evaluated at  $\hat{t} = h$ , giving

$$z_k(t_{n+1}) = A_k e^{-\lambda_k h} + B_k + C_k h$$

By expanding the coefficients  $A_k, B_k$  and  $C_k$ , the general solution can be matched to the update formula obtained using linear interpolation for forcing function given in (A.2)

## BIBLIOGRAPHY

1. Thomas J.R. Hughes. *The Finite Element Method: Linear Static and Dynamic Finite Element Analysis*. Dover Publication, Inc., 2000.
2. Prapot Kunthong and Lonny L. Thompson. An efficient solver for the high-order accurate time-discontinuous galerkin (TDG) method for second-order hyperbolic systems. *Finite Elements in Analysis & Design*, 141(7-8):729–762, 2005.
3. Lonny L. Thompson and Prapot Kunthong. Stabilized time-discontinuous galerkin methods with applications to structural acoustics. In *Paper IMECE2006-15753, Proceedings IMECE'06*, Chicago, Illinois, Nov. 5-10 2006. The American Society of Mechanical Engineers. 2006 International Mechanical Engineering Conference & Exposition.
4. T. K. Hasselman. Modal coupling in lightly damped systems. *AIAA Journal*, 14(11):1627-1628, 1976.
5. E.E. Henkel and R. Mar. Transient solution of coupled structural components using system modal coordinates with and without coupled system damping. *Proceedings of Damping '93 Conference*, 1993.
6. J.M. Chapman. Incorporating a full damping matrix in the transient analysis of nonlinear structures. *Proceedings of Damping '93 Conference*, 1993.
7. C.P. Fritzen. Identification of mass, damping and stiffness matrices of mechanical systems. *ASME J. Vibr. Acoust.*, 108:9–16, 1986.
8. S. Naylor, M.F. Platten, J.R. Wright, and J.E. Cooper. Identification of multi-degree of freedom systems with nonproportional damping using the resonant decay method. *Journal of Vibration and Acoustics*, 126(2):298–306, 2004.
9. L. Kefu, M.R. Kujath, and W. Zheng. Quantification of non-proportionality of damping in discrete vibratory systems. *Computers and Structures*, 77:557–569, 2000.
10. U. Prells and M.I. Friswell. Measure of non-proportional damping. *Mechanical Systems and Signal Processing*, 14:125–137, 2000.
11. J.A. Fromme and Michael A. Golberg. Transient response analysis of nonlinear modally coupled structural dynamics equations of motion. *AIAA Journal*, 36(8):1486–1493, 1998.

12. K.A. Foss. Coordinates which uncouple the equations of motion of damped linear dynamic systems. *Proceedings of ASME Annual Meeting, American Society of Mechanical Engineers, New York, (Paper 57-A-86)*, 1957.
13. W.C. Hurty and M.F. Rubinstein. *Dynamics of Structures*. Prentice-Hall, 1964.
14. L. Meirovitch. *Fundamentals of Vibrations*. McGraw-Hill, 2001.
15. John Dickens. Exact solution for coupled (non-proportional) damping time history response. *Proceedings of the 2003 Spacecraft and Launch Vehicle Dynamic Environments Workshop, The Aerospace Corporation, El Segundo, CA, June 17-19, 2003*.
16. R.R. Jr. Craig. *Structural Dynamics, An Introduction to Computer Methods*. John Wiley & Sons, 1981.
17. D.M. Trujillo. The direct numerical integration of linear matrix differential equations using Pade approximations. *International Journal for Numerical Methods in Engineering*, 9:259–270, 1975.
18. C. Moler and Van Loan C. *Numerical Linear Algebra Techniques for Systems and Control*. IEEE Press, IEEE Control Systems Society, 1994.
19. Hans M. Hilber, Thomas J. R. Hughes, and Robert L. Taylor. Improved numerical dissipation for time integration algorithms in structural dynamics. *Earthquake Engineering and Structural Dynamics*, 5:283–292, 1977.
20. R.A. Frazer, W.J. Duncan, and A.R. Collar. *Elementary Matrices*. The Macmillan Company, New York, 1946.
21. D.L. Cronin. Numerical integration of uncoupled equations of motion using recursive digital filtering. *International Journal for Numerical Methods in Engineering*, 6:137–140, 1973.
22. L.F. Shampine, R.C. Allen, and S. Pruess. *Fundamentals of Numerical Computing*. John Wiley & Sons, Inc., 1997.
23. A. Mũgan. Discrete equivalent time integration methods for transient analysis. *International Journal for Numerical Methods in Engineering*, 57:2043–2075, 2003.